Astronomy Reports, Vol. 48, No. 11, 2004, pp. 900–908. Translated from Astronomicheskiĭ Zhurnal, Vol. 81, No. 11, 2004, pp. 988–997.

Quasi-Simultaneous VLBI and RATAN-600 Observations of Active Galactic Nuclei

A. B. Pushkarev[1], Yu. Yu. Kovalev[2,3], I. E. Molotov[1], M. B. Nechaeva[4], Yu. N. Gorshenkov[5], G. Tuccari[6], C. Stanghellini[6], X. Hong[7], J. Quick[8], S. Dougherty[9], and X. Liu[10]

[1]*Main Astronomical Observatory, Russian Academy of Sciences, Pulkovo, St.Petersburg, 196140 Russia*

[2]*National Radio Astronomy Observatory, P.O. Box 2, Rt. 28/92, Green Bank, WV 24944-0002, USA*

[3]*AstroSpace Center of the Lebedev Institute of Physics, Russian Academy of Sciences, Profsoyuznaya ul. 84/32, Moscow 117997, Russia*

[4]*Radiophysical Research Institute, ul. Bol'shaya Pecherskaya 25/14, Nizhni Novgorod, 603600 Russia*

[5]*Special Design Bureau, Power Engineering Institute, Krasnokazarmennaya ul. 14, Moscow, 111250 Russia*

[6]*Istituto di Radioastronomia del C.N.R., Stazione VLBI di Noto, C. da Renna Bassa – Loc. Case di Mezzo, C.P. 141, 96017 Noto (SR), Italy*

[7]*Shanghai Astronomical Observatory, 80 Nandan Road, Shanghai 200030, China*

[8]*Hartebeesthoek Radio Astronomy Observatory, P.O. Box 443, Krugersdorp 1740, South Africa*

[9]*Dominion Radio Astrophysical Observatory, P.O. Box 248, Penticton, B.C. V2A 6K3, Canada*

[10]*Urumqi Astronomical Observatory, 40-5 South Beijing Road, Urumqi, Xinjiang 830011, China*

Received March 10, 2004; in final form, May 27, 2004

Abstract—VLBI observations of several quasars and BL Lacertae objects were carried out at 1.66 GHz in November–December 1999 using six antennas (Medvezh'i Ozera, Svetloe, Pushchino, Noto, HartRAO, and Shanghai). Maps of six sources (0420+022, 0420–014, 1308+326, 1345+125, 1803+784, and DA 193) obtained with milliarcsecond resolution are presented and discussed, together with their broadband (1–22 GHz) spectra obtained on the RATAN–600 radio telescope at epochs close to those of the VLBI observations. Comparison of the VLBI maps with maps of these sources obtained on standard VLBI networks and with the RATAN–600 quasi-simultaneous total-flux measurements indicates the reliability of the results obtained on this Low Frequency VLBI Network and the good efficiency of this network.

1. INTRODUCTION

The Low Frequency VLBI Network (LFVN) project has been in operation since 1996 [1]. Its main goal is to help organize international VLBI experiments at low frequencies with the participation of Russian radio telescopes. During this time, 13 antennas have been equipped with the necessary radio astronomy receivers and data acquisition instrumentation: the Medvezh'i Ozera (64 m), Pushchino (22 m), Zimenki (15 m), and Staraya Pustyn' (14 m) telescopes in Russia, the Evpatoria (70 m) and Simeiz (22 m) telescopes in the Ukraine, as well as the Ventspils (32 m, Latvia), Noto (32 m, Italy), Toruń (14 m, Poland), Pune (45 m, India), Urumqi (25 m, China) and Shanghai (25 m, China) antennas and the Ooty 500×30 parabolic cylinder (India). Eighteen VLBI experiments using various combinations of radio telescopes located in England, India, Italy, Canada, China, Latvia, Poland, Russia, USA, Ukraine, South Africa, and Japan were organized, as well as correlation centers in Canada, Russia, and the USA.

At present, three aspects of the LFVN project are being developed: (1) a subsystem based on a Mk-2 data acquisition terminal and the NIRFI-3 correlator in Nizhniĭ Novgorod for studies of the solar wind and solar microflares (spikes) at 327 MHz and 610 MHz; (2) an international network based on the S2 broadband Canadian recording terminal [2, 3] and the Dominion Radio Astronophysical Observatory (DRAO) correlator at Penticton (Canada) [4] for studies of active galactic nuclei, maser sources, and active stars at 1.66 and 4.82 GHz; and (3) VLBI radar at 5010 MHz with retransmission of the received echo signals to the Noto processing center [5] via the Internet for measurements of the motions of the terrestrial planets, asteroids approaching the Earth, and so-called "space garbage."

1063-7729/04/4811-0900$26.00

The international network of radio telescopes equipped with S2 recorders included the Medvezh'i Ozera, Svetloe (32 m), Pushchino telescopes in Russia, the Green Bank (43 m) and Arecibo (300 m) telescopes in the USA, and the Noto (Italy), HartRAO (26 m, South Africa), and Shanghai (China) telescopes. Since 1998, the experiments INTAS98.2, INTAS98.5, INTAS99.4, INTAS00.3, and LFVN03.1 have been performed at 18 cm. The first four of these have been successfully correlated on the Penticton correlator; our results for INTAS99.4 are presented and discussed in this paper. The results for the other experiments will appear in subsequent publications.

In this paper, we will use the values of the Hubble constant $H_0 = 70h$ km s^{-1} Mpc^{-1} and the deceleration parameter $q_0 = 0.5$.

2. OBSERVATIONS AND REDUCTION

The LFVN observations were carried out from November 30 to December 3, 1999 (epoch 1999.91), at a frequency of 1.66 GHz. The total duration of the experiment was 43 h, with a mean duration for each scan of about 30 min. Each of sources was observed in 5–8 scans. Figure 1 shows the resulting coverage of the (u, v) plane for DA 193 as an example.

The Medvezh'i Ozera, Pushchino, Svetloe, Noto, Shanghai, and HartRAO antennas participated in the experiment. Some parameters of the radio telescopes communicated to us by the staff of the observatories are listed in Table 1 (diameter, system temperature, and system equivalent flux density, SEFD). The participation of the HartRAO antenna (South Africa) considerably improved the angular resolution in the north–south direction. The maximum projected baseline between Shanghai and HartRAO reached 10 170 km. The Canadian S2 data acquisition system was used. The bandwidth was 4 MHz (256 spectral channels, each 15.625 kHz). Left-circular polarization was recorded with one-bit signal sampling. The correlation of the data was performed on the DRAO correlator in Penticton with an averaging time of 2 s.

The data analysis, editing, calibration, and imaging (for more details, see [6]) were done using standard procedures in the AIPS package (NRAO). For the amplitude calibration of the data, we used gain curves and system temperatures measured for each of the antennas involved in the observations. The primary phase calibration was done using the AIPS task FRING with a coherent integration time of 120 s, with subsequent phase corrections for the residual delays being found for the entire time of the experiment, with the Medvezh'i Ozera telescope used as the reference antenna. A point source at the phase center was used for the initial models in the hybrid mapping.

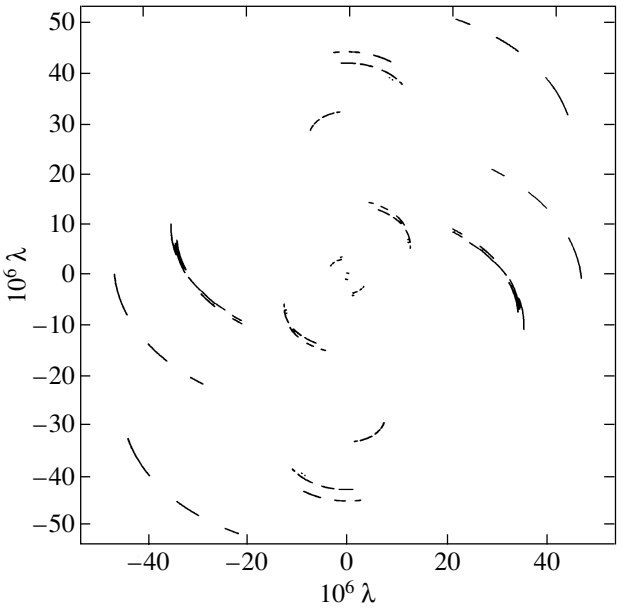

Fig. 1. Coverage of the (u, v) plane for DA 193 for LFVN observations at 18 cm.

The observations of the broadband spectra of the sources were carried out as part of an ongoing program of monitoring of compact extragalactic objects on the largest Russian radio telescope – the RATAN-600 (Special Astrophysical Observatory, Russian Academy of Sciences). A description of this program, the procedure used for the observations, and the data processing are given by Kovalev *et al.* [7].

3. DISCUSSION

Our results for six extragalactic objects are presented below. Figures 2–7 show the LFVN maps together with the broadband spectra of the sources obtained on the RATAN-600 at epochs close to the date of the VLBI experiment. We have modeled the VLBI

Table 1. Antennas and their parameters at 1.66 GHz

Antenna	Diameter, m	T_{sys}, K	SEFD, Jy
Svetloe (Russia)	32	71	394
Medvezh'i Ozera (Russia)	64	95	156
Pushchino (Russia)	22	111	1586
HartRAO (South Africa)	26	50	500
Noto (Italy)	32	107	1070
Shanghai (China)	25	100	1250

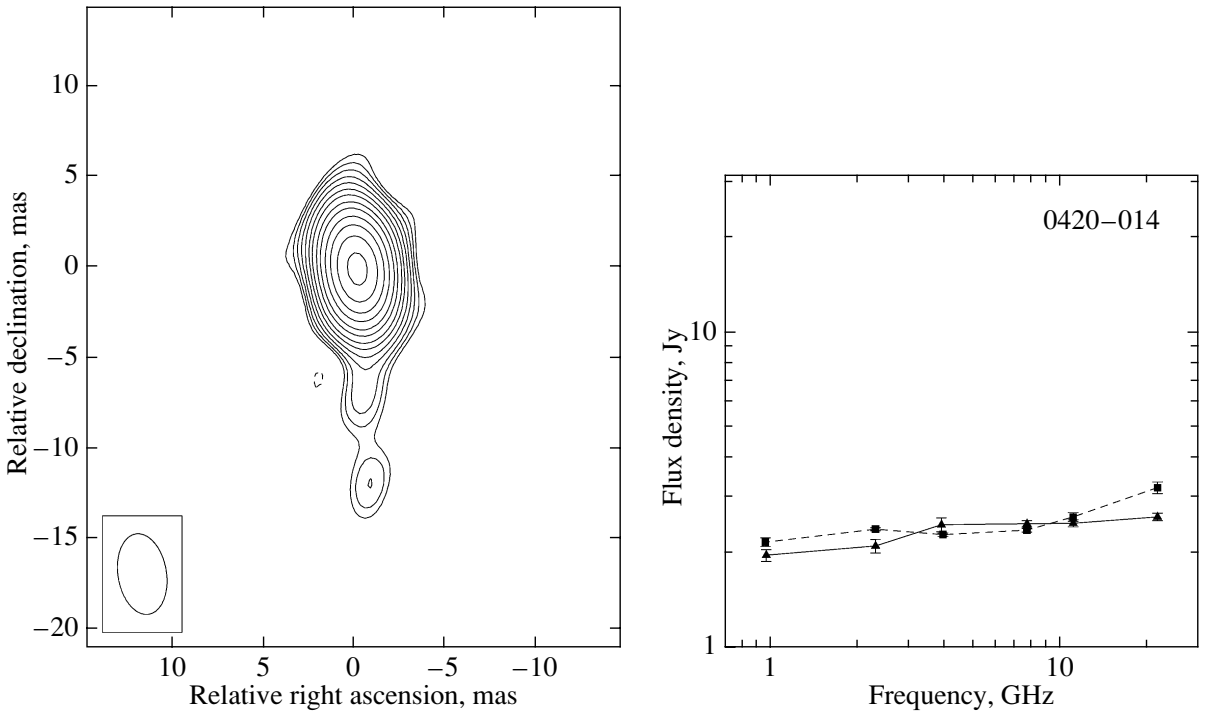

Fig. 2. Left: 1.66-GHz LFVN map of 0420−014. The lowest contour is drawn at a level of 1.4% of the peak value of 1370 mJy/beam, and the contours increase in steps of $\sqrt{2}$. The restoring beam is 3.6×2.2 mas in position angle $-8°$. Right: the broadband spectrum measured on the RATAN-600. Individual measurements are shown with $\pm 1\sigma$ errors and are connected with lines. The filled triangles and solid line segments show the measurements for September 1999, and the filled squares and dashed line segments those for April 2000.

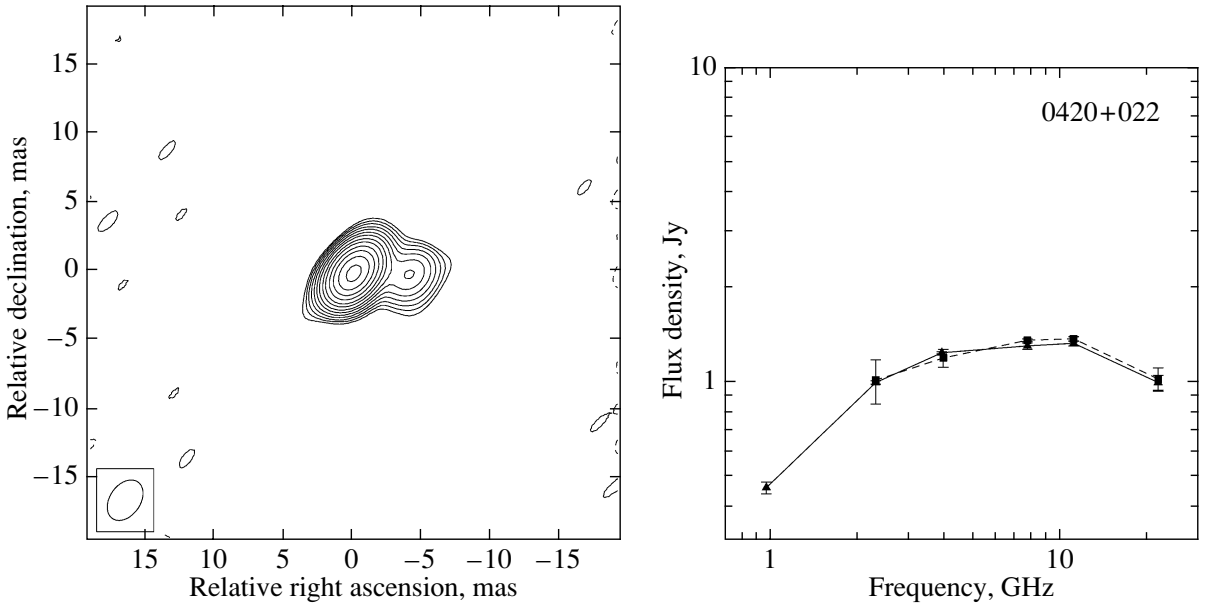

Fig. 3. Left: 1.66-GHz LFVN map of 0420+022. The lowest contour is drawn at a level of 1.4% of the peak value of 775 mJy/beam, and the contours increase in steps of $\sqrt{2}$. The restoring beam is 3.2×2.2 mas in position angle $-35°$. Right: same as Fig. 2b for 0420+022.

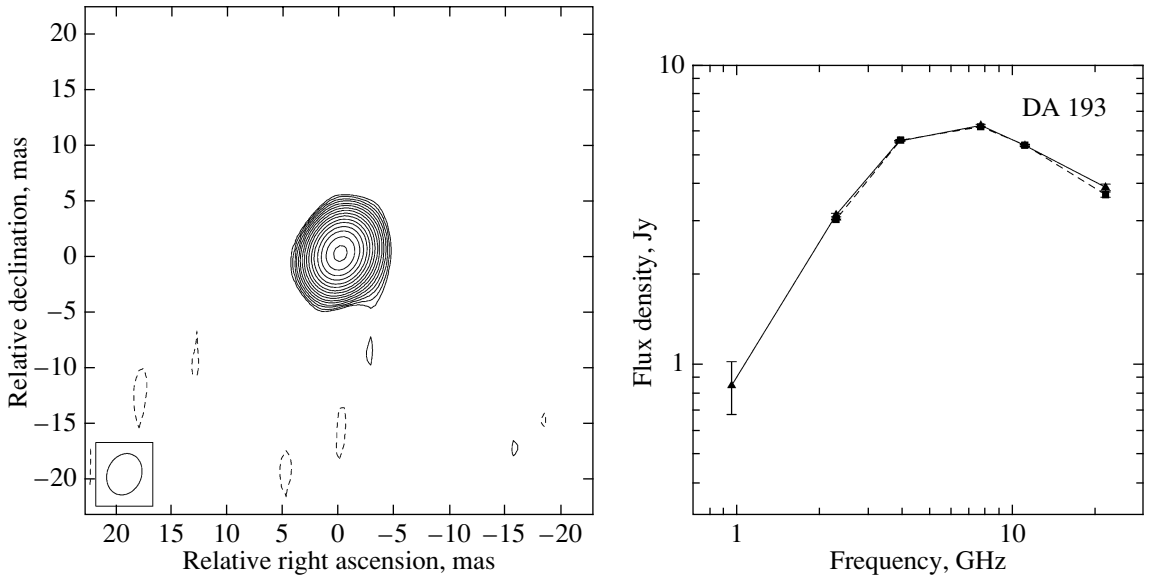

Fig. 4. Left: 1.66-GHz LFVN map of DA 193 (0552+398). The lowest contour is drawn at a level of 0.5% of the peak value of 1833 mJy/beam, and the contours increase in steps of $\sqrt{2}$. The restoring beam is 3.7 × 3.0 mas in position angle −48°. Right: same as Fig. 2b for DA 193.

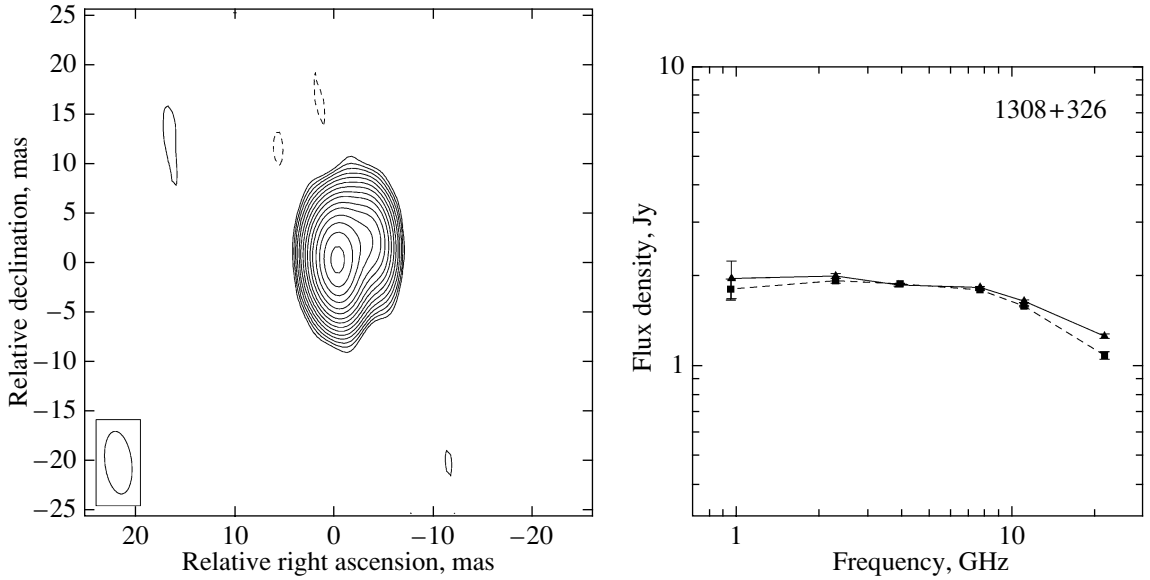

Fig. 5. Left: 1.66-GHz LFVN map of 1308+326. The lowest contour is drawn at a level of 0.7% of the peak value of 1565 mJy/beam, and the contours increase in steps of $\sqrt{2}$. The restoring beam is 6.2 × 2.6 mas in position angle +8°. Right: same as Fig. 2b for 1308+326.

structures of the sources with circular Gaussian components by fitting the models to the fully calibrated observational data in the visibility (u, v) plane using the Brandeis VLBI package [8]. The source models are listed in Table 2, which gives the (1) object name, (2) total flux density of the model component, (3)–(4) component position on the map in polar coordinates r and φ relative to the brightest component, (5) the FWHM of the Gaussian component. The formal errors are given at the 1σ level; this corresponds to an increase in the value of χ^2 for the obtained model by unity (for details see [9]). For the object 1345+125, which has a composite structure, it was not possible to derive an adequate model of the source due to the sparse coverage of the (u, v) plane.

Let us proceed to a discussion of each of the studied objects.

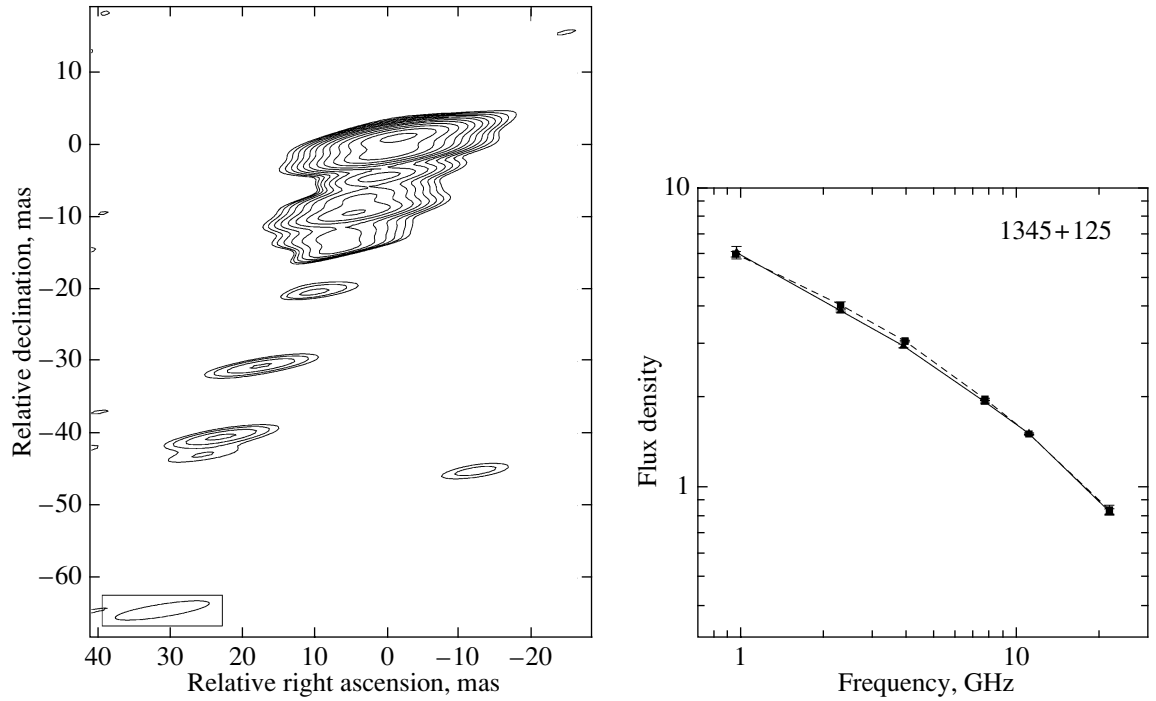

Fig. 6. Left: 1.66-GHz LFVN map of 1345+125. The lowest contour is drawn at a level of 5.6% of the peak value of 515 mJy/beam, and the contours increase in steps of $\sqrt{2}$. The restoring beam is 12.1×1.8 mas in position angle $-82°$. Right: same as Fig. 2b for 1345+125.

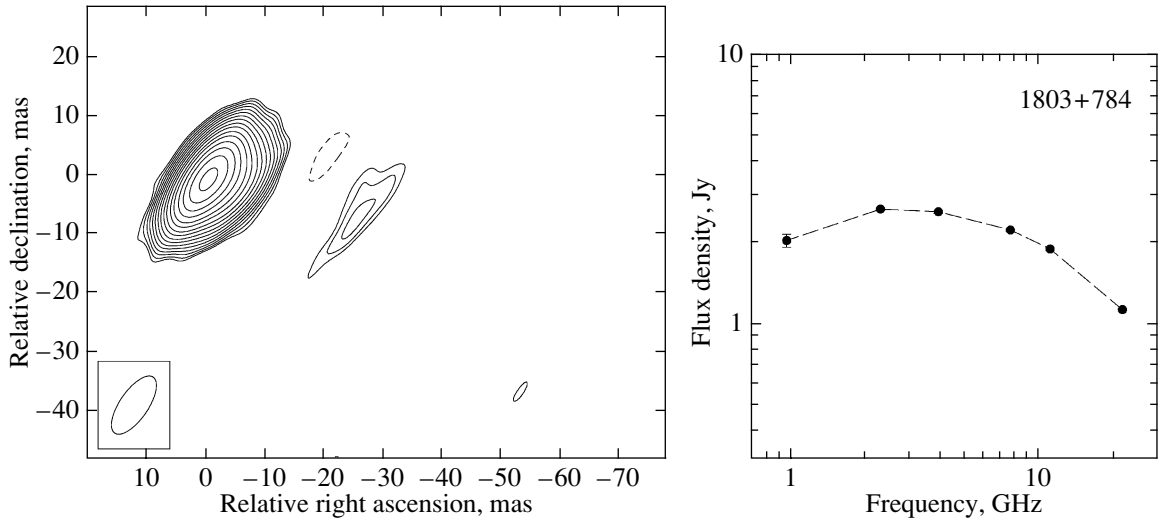

Fig. 7. Left: 1.66-GHz LFVN map of 1803+784. The lowest contour is drawn at a level of 0.5% of the peak value of 1480 mJy/beam, and the contours increase in steps of $\sqrt{2}$. The restoring beam is 11.5×4.8 mas in position angle $-34°$. Right: same as Fig. 2b for 1803+784, but for measurements made in September 1998.

0420−014. This source is a strongly variable and highly polarized quasar (redshift $z = 0.915$) with a flat radio spectrum (Fig. 2). 0420−014 was identified with a gamma-ray source based on analysis of Compton Gamma-Ray Observatory EGRET data [10, 11]. In 1992, simultaneous optical and gamma-ray flares were observed together with a considerable increase of the radio emission, which was subsequently identified with the appearance of a new component in the jet. Analysis of the data for the 1992 flare suggest the presence of a binary black hole in this source [12].

Our map of 0420−014 demonstrates a dominant VLBI core and several weak components in the southward jet (Fig. 2). The morphology of

Table 2. Models of the sources

Source	$I \pm \sigma_I$, mJy	$r \pm \sigma_r$, mas	$\varphi \pm \sigma_\varphi$, deg	$\theta \pm \sigma_\theta$, mas
0420−014	1309 ± 42	...	...	<0.5
	110 ± 23	1.78 ± 0.12	159 ± 5.5	<0.5
	30 ± 4	7.06 ± 0.22	-176 ± 0.7	<0.5
	20 ± 5	12.59 ± 0.38	-176 ± 0.8	<0.5
0420+022	772 ± 28	...	...	<0.5
	52 ± 9	1.78 ± 0.14	-41 ± 4.6	<0.5
	61 ± 8	2.31 ± 0.21	-86 ± 4.8	0.63 ± 0.25
	73 ± 8	4.53 ± 0.25	-93 ± 3.3	<0.64
DA 193	1872 ± 8	...	...	0.55 ± 0.05
1308+326	1389 ± 44	...	...	1.11 ± 0.10
	925 ± 68	2.33 ± 0.13	35 ± 3.1	1.97 ± 0.23
	299 ± 60	4.99 ± 0.15	54 ± 1.8	1.45 ± 0.61
1803+784	1459 ± 87	...	...	1.10 ± 0.26
	80 ± 16	2.80 ± 0.23	-100 ± 4.1	0.89 ± 0.31
	322 ± 31	4.83 ± 0.46	-104 ± 5.2	1.99 ± 0.88
	36 ± 9	26.24 ± 0.87	-103 ± 1.2	1.18 ± 0.35

the source on kiloparsec scales shows a similar southward core–jet structure [13]. The jet compnent closest to the VLBI core, at an angular distance of 1.78 mas from the core (Table 2), can be identified with a feature observed in October 1995 (1995.83) at 5 GHz [14]. The proper motion of the component is $\sim$0.035 mas year^{-1}, which corresponds to an apparent projected linear speed of $\beta_{\rm app} = 1.3h^{-1}$. The speed of this component between 1992 and 1995 was higher, $\beta_{\rm app} = 4.1h^{-1}$ [14]; this is consistent with the possibility that the jet is decelerated, with the speed of the VLBI component decreasing with distance from the core.

0420+022. 0420+022, which has a flat radio spectrum (Fig. 3), was originally classified as a probable BL Lacertae object [15]. However, its redshift was soon found to be $z = 2.28$ [16]. Such a large of redshift is not typical of BL Lacertae objects, whose redshifts, as a rule, do not exceed unity [17]. Following [16], we will consider this source to be a quasar.

RATAN-600 monitoring of the broadband spectrum of this object revealed unusual variability. In some time intervals (on scales of months), strong variability of the total flux density at frequencies below 10 GHz was observed together with weak variability above this frequency, with the variability amplitude increasing with decreasing frequency. VLBI observations were carried out to identify the mechanism responsible for the observed atypical variability. A detailed analysis of this behavior incorporating the results presented here and other VLBI and RATAN-600 observations will appear in a forthcoming paper by Yu.Yu. Kovalev *et al*.

The LFVN map of the source (Fig. 3) reveals a core–jet structure on milliarcsecond scales. The jet extends westward to a projected distance of about 5 mas ($\sim$28 pc) at a level of about 10 mJy.

DA 193. The variable quasar 0552+398 (DA 193, $z = 2.36$) is classified as a GPS source [18], reflecting the fact that its broadband radio spectrum peaks at decimeter–centimeter waves (Fig. 4). DA 193 was observed as a calibrator in our VLBI observations; it is one of the most compact radio sources currently known. Figure 1 shows the (u, v) plane coverage for this source obtained in INTAS99.4. Our 1.66-GHz observations do not detect any jet emission — only a "naked" 0.55-mas VLBI core (Fig. 4). The westward VLBI jet becomes visible at 5 GHz [14] and higher frequencies. The jet components' speeds measured using 43 GHz VLBI maps turn out to be superluminal, which is not typical of GPS sources [19].

1308+326. This variable, flat-spectrum source ($z = 0.996$; Fig. 5) belongs to a complete sample of radio-bright northern BL Lacertae objects [20], although there are reasons to suppose that the

source should, in fact, be classified as a quasar [21]. 1308+326 is a candidate microlensed object. The structure of 1308+326 on kiloparsec scales represents a bright core, a component ∼11" to the north, and a fainter component ∼6" to the east [22].

In our experiment, this object was observed to link the emission detected on arcsecond (kiloparsec) and milliarcsecond (parsec) scales. The image (Fig. 5) shows that the source structure at 18 cm is compact, consisting of a VLBI core and two jet components, with the outer component lying 5 mas (30 pc) to the northwest of the core ($\varphi = 54°$). Thus, the jet we have detected is too short to trace the outflow direction on intermediate scales; it may be possible to image this structure using an array with a combination of relatively long and small VLBI baselines (for example, the EVN+MERLIN or the VLBA+NMA).

1345+125. This object ($z = 0.122$) is one of the nearest bright GPS sources (Fig. 6). The host galaxy contains a western and eastern component. The radio source 1345+125 is identified with the western component, which is an elliptical galaxy [23]. We may be observing the merger of two galaxies, which stimulates the activity at radio frequencies [24].

The observations of this object were of interest from the point of view of its classification: it is probably a compact symmetrical object (CSO). Sources of this class are powerful and compact objects with a total size not larger than one kiloparsec. As a rule, the emission is dominated by regions of the jet and hot spots on either sides of the "central engine," and these sources are probably not subject to considerable Doppler brightening [25]. The small sizes of these sources may be a consequence of their youth ($< 10^4$ years). This hypothesis was confirmed after the detection of motions of the hot spots in CSO sources and estimation of their speedss [26]. Most identified CSO sources are also classified as GPS objects based on their broadband radio spectra. Due to the high compactness of these objects, their structure can be resolved only by VLBI observations.

Our 18-cm map of 1345+125 displays a very rich structure. The VLBI jet is detected to distances of up to 50 mas (103 pc) to the southeast of the core in position angle ∼150°. According to Fey *et al.* [27], the core is not detected at 1.6 GHz because of strong self-absorption in the circumnuclear region. Our observations confirm the results of (EVN+GEO) observations of 1345+125 at 8.4, 2.3, and 1.6 GHz [28], and the conclusion that this object is a CSO source. Unfortunately, the lack of data for this source on the short Medvezh'i Ozera–Pushchino baseline has hindered the detection of emission from the most extended regions of the source [29]; in turn, this has resulted in a considerable underestimation of its integrated flux (Table 3).

1803+784. This flat-spectrum source (Fig. 7) is a BL Lacertae object, and is included in the 1-Jy catalog of such objects [20] ($z = 0.68$ [30]).

The purpose of our observations of 1803+784 was to study the structure of this BL Lacertae object and to link the source morphology on parsec and kiloparsec scales. Maps on kiloparsec scales [31, 32] demonstrate the presence of two extended components, one located 2" to the southwest of the core and the other, weaker, component located approximately 45" in position angle $\sim -165°$; there is also very faint emission between these features [33, 34]. The total size of the observed radio structure is ∼180 kpc. On the other hand, VLBI observations with the HALCA orbiting radio telescope [35] made it possible to study the subparsec structure of the source and the direction of the VLBI jet at ∼0.5 mas, close to the central engine. The jet extends first to the northwest in position angle $\sim -65°$ and then turns to the southwest [36].

Figure 7 shows our 18-cm LFVN map of the object. The source has a number of jet components to the southwest of the core in position angle $\sim -100°$. The most distant component detected on our map is 26 mas (143 pc) from the core. The jet direction and the location of this component are consistent with the results obtained on a more sensitive network (VLBA, VLA, Goldstone) at epoch 1998.55 [37].

Thus, 1803+784 displays a considerable difference in the projected jet directions on parsec and kiloparsec scales (∼100° in the plane of the sky). This can be explained by the effect of projection or interaction of the jet with the surrounding medium.

Modeling of the broadband spectra presented in this paper (see details in [38]) and literature data for VLA observations of these sources indicate the presence of extended radio structure in half of these objects. Table 3 lists the total fluxes of the sources from the LFVN maps and the total fluxes obtained by interpolating the RATAN-600 data. Based on the accuracy of the calibration curves and system temperatures used, the total uncertainties in the integrated fluxes on VLBI scales are ≈10%. We estimate the uncertainties in the total flux densities for the RATAN-600 data to be not larger than 5% (allowing for uncertainties in the interpolation and the measurements themselves; Figs. 2–7).

The excess of the integrated fluxes from the VLBI maps (decaparsec scales) above the RATAN-600 flux densities for 0420+022 and 1308+326 could be due to inaccuracy of the LFVN amplitude calibration and by the fact that the VLBI and RATAN-600 observations were not strictly simultaneous (the minimum interval between the two sets of observations was two months). This may also play some role for 0420+022,

Table 3. Comparison of the total flux densities of the sources measured on the LFVN and the RATAN-600

Instrument	Total flux density at 18 cm, Jy					
	0420−014	0420+022	DA 193	1308+326	1345+125	1803+784
RATAN-600*	2.0	0.76	1.9	2.0	4.7	<2.4
LFVN	1.5[1]	0.96	1.9	2.6	2.0	1.9[2]

* Values obtained by interpolating the 31- and 13-cm data.
[1] The source is significantly resolved on kiloparsec scales.
[2] The epochs of the LFVN and RATAN-600 observations differ by 1 year.

which is variable at low frequencies (this will be described in more detail in a forthcoming paper by Yu.Yu. Kovalev *et al.*).

4. CONCLUSION

We have presented the results of observations of six extragalactic radio sources on the Low Frequency VLBI Network, involving three Russian and three foreign radio telescopes. we have restored the intensity distributions of the objects with millisecond angular resolution by processing the data using the standard method and with the standard software package. We have discussed our results in the context of our the broadband RATAN-600 spectral observations and previously published EVN and VLBA maps. Comparison of our maps with those from other studies indicates the reliability of the LFVN images and the efficiency of the LFVN. It is desirable to refine the calibration curves of some of the LFVN telescopes to improve the accuracy of the amplitude calibration of the data.

We have also obtained positive experience in connection with planning and realizing VLBI experiments. Using the available fully steerable Russian radio telescopes in these experiments helped to maintain them in working condition and to equip them with new radio astronomical instrumentation. The collaboration between the Russian and foreign observatories and the correlation centers allows the Low Frequency VLBI Network to carry out yearly observating sessions aimed at acquiring data for the solution of a broad variety of scientific problems, including observations of active galactic nuclei.

ACKNOWLEDGMENTS

This work was supported by INTAS (grants 96-0183, 2001-0669), the NSFC (grant 19973014), and the Russian Foundation for Basic Research (project code 03-02-27173). The RATAN-600 measurements were partially supported by the Federal Science and Technology Program in Astronomy (grant 1.2.5.1), the Ministry of Industry, Science, and Technology of the Russian Federation under subcontract to the Special Astrophysical Observatory with the Astro Space Center of the Lebedev Physical Institute, and the Russian Foundation for Basic Research (project code 02-02-16305). Yu.Yu. Kovalev participated in this work as an NRAO Karl Jansky Postdoctoral Fellow. The authors thank the staff of the observatories and of the Penticton correlation center who made this experiment possible.

REFERENCES

1. I. E. Molotov, S. F. Likhachev, A. A. Chuprikov, *et al.*, *The Universe at Low Radio Frequencies*, Ed. by A. Pramesh Rao, G. Swarup, and Gopal-Krishna, IAU Publ. **199**, 492 (2002).
2. R. D. Wietfeldt, D. Baer, W. H. Cannon, *et al.*, IEEE Trans. Instrum. Meas. **45**, 923 (1996).
3. W. H. Cannon, D. Baer, G. Feil, *et al.*, Vistas Astron. **41**, 297 (1997).
4. B. R. Carlson, P. E. Dewdney, T. A. Burgess, *et al.*, Publ. Aston. Soc. Pac. **111**, 1025 (1999).
5. G. Tuccari, I. Molotov, S. Buttaccio, *et al.*, *Booklet of the 3rd IVS General Meeting*, Ottawa, 2004 (Geodetic Survey Div., Natural Resources Canada, 2004), p. 40.
6. A. R. Thompson, J. M. Moran, and G. W. Swenson, Jr., *Interferometry and Synthesis in Radio Astronomy* (Wiley, 2001; Fizmatlit, Moscow, 2003).
7. Y. Y. Kovalev, N. A. Nizhelsky, Yu. A. Kovalev, *et al.*, Astron. Astrophys., Suppl. Ser. **139**, 545 (1999).
8. D. C. Gabuzda, T. V. Cawthorne, D, H. Roberts, and J. F. C. Wardle, Astrophys. J. **347**, 701 (1989).
9. D. H. Roberts, J. F. C. Wardle, and I. F. Brown, Astrophys. J. **427**, 718 (1994).
10. J. R. Mattox, R. C. Hartman, and O. Reimer, Astrophys. J., Suppl. Ser. **135**, 155 (2001).
11. D. Sowards-Emmerd, R. W. Romani, and P. F. Michelson, Astrophys. J. **590**, 109 (2003).
12. S. Britzen, A. Witzel, T. P. Krichbaum, *et al.*, Astron. Astrophys. **360**, 65 (2000).
13. R. R. J. Antonucci and J. S. Ulvestad, Astrophys. J. **294**, 158 (1985).
14. X. Y. Hong, T. Venturi, T. S. Wan, *et al.*, Astron. Astrophys. **134**, 201 (1999).
15. M. P. Veron-Cetty and P. Veron, Astron. Astrophys. **412**, 399 (2003).

16. S. L. Ellison, L. Yan, I. M. Hook, *et al.*, Astron. Astrophys. **379**, 393 (2001).
17. M. Stickel, J. W. Fried, and H. Kühr, Astron. Astrophys., Suppl. Ser. **98**, 393 (1993).
18. C. P. O'Dea, S. A. Baum, and C. Stanghellini, Astrophys. J. **380**, 66 (1991).
19. L. M. Lister, A. P. Marscher, and W. K. Gear, Astrophys. J. **504**, 702 (1998).
20. M. Stickel, P. Padovani, C. M. Urry, *et al.*, Astrophys. J. **374**, 431 (1991).
21. D. C. Gabuzda, R. I. Kollgaard, D. H. Roberts, and J. F. C. Wardle, Atrophys. J. **410**, 39 (1993).
22. D. W. Murphy, I. W. A. Browne, and R. A. Perley, Monthly Notices Roy. Astron. Soc. **264**, 298M (1993).
23. N. A. Shaw, A. K. Tzioumis, and A. Pedlar, Mon. Not. R. Astron. Soc. **256**, 6 (1992).
24. T. M. Hechman, E. P. Smith, and S. A. Baum, Astrophys. J. **311**, 526 (1986).
25. P. N. Wilcinson, A. G. Polatidis, A. C. S. Readhead, *et al.*, Astrophys. J. **432**, L87 (1994).
26. I. Owsianik and J. E. Conway, Astron. Astrophys. **337**, 69 (1998).
27. A. L. Fey, A. W. Clegg, and E. B. Fomalont, Astrophys. J. **105**, 299 (1996).
28. L. Xiang, C. Stanghellini, D. Dallacasa, and Z. Haiyan, Astron. Astrophys. **385**, 768 (2002).
29. M. L. Lister, K. I. Kellermann, R. C. Vermeulen, *et al.*, Astrophys. J. **584**, 135 (2003).
30. A. Witzel, C. J. Schalinski, K. J. Johnston, *et al.*, Astron. Astrophys. **206**, 245 (1988).
31. R. R. J. Antonucci, P. Hickson, E. W. Olszewski, and J. S. Miller, Astrophys. J. **92**, 1 (1986).
32. R. I. Kollgaard, D, H. Roberts, J. F. C. Wardle, and D. C. Gabuzda, Astron. J. **104**, 1687 (1992).
33. R. G. Strom and P. L. Bierman, Astron. Astrophys. **242**, 313 (1991).
34. P. Cassaro, C. Stanghellini, M. Bondi, *et al.*, Astron. Astrophys. **139**, 601 (1999).
35. H. Hirabayashi, H. Hirosava, H. Kobayashi, *et al.*, Publ. Astron. Soc. Jpn. **52**, 955 (2000).
36. D. C. Gabuzda, New Astron. Rev. **43**, 691 (1999).
37. D. C. Gabuzda and V. A. Chernetskii, Mon. Not. R. Astron. Soc. **339**, 669 (2003).
38. Y. Y. Kovalev, Y. A. Kovalev, N. A. Nizhelsky, and A. V. Bogdantsov, Publ. Astron. Soc. Austral. **19**, 83 (2002).

Translated by G. Rudnitskiĭ